On the Precession of Quasi-Equatorial, Quasi-Circular Geodesics in Kerr Spacetime

Lorenz Zwick
ETH Zürich

June 1, 2018

Abstract

The aim of this paper is to analyse geodetic motion in first order near to the equatorial plane of a Kerr black hole. We briefly describe the dynamics in the equatorial plane and proceed to solve the radial equation of motion with a harmonic approximation of the effective potential. We recover the Schwarzschild and Kerr precession terms for a semi-Newtonian orbit. Next, we use the geodesic equation to find a linearised equation of motion that couples radial oscillations to the azimuthal angle. We find an interesting interaction between radial and azimuthal oscillations that results in a complex precession of the orbital angular momentum.

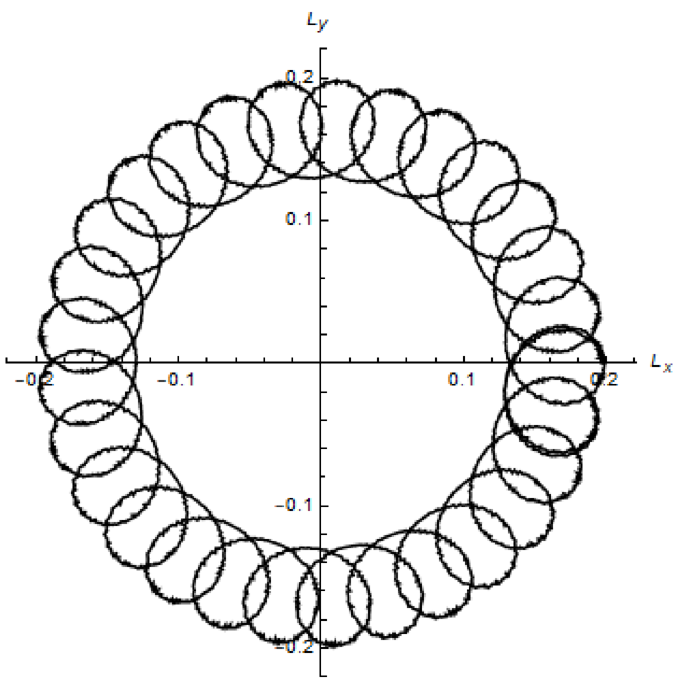

Contents

1 Introduction

1.1 The Kerr Metric

Found by Roy Kerr in 1963, the Kerr metric is the most general stationary and axis-symmetric solution of the Einstein field equations for empty space [1]. For the scope of this work, we will assume that it accurately describes space-time around a rotating black hole.

A black hole of mass M and angular momentum J is characterised by two parameters: the Schwarzschild radius $r_s = 2GMc^{-2}$ and the spin $a = JM^{-1}c^{-1}$, where G_0 is Newton's gravitational constant and c is the speed of light. In spherical coordinates (t, r, θ, ϕ) aligned with the axis of rotation, the line element of the metric assumes the characteristic form [2]:

$$ds^2 = (1 - \frac{rr_s}{\rho^2})dt^2 + 2\frac{rr_s a}{\rho^2}sin(\theta)^2 dt d\phi - \frac{\Sigma^2}{\rho^2}sin(\theta)^2 d\phi^2 - \frac{\rho}{\Delta}dr^2 - \rho^2 d\theta^2 \tag{1}$$

where we define various variables:

$$\rho^2 = r^2 + a^2 cos(\theta)^2$$
$$\Delta = r^2 - rr_s + a^2$$
$$\Sigma^2 = (r^2 + a^2)^2 - a^2\Delta sin(\theta)^2$$

Note that we are using natural units where the speed of light $c = 1$ and the gravitational constant $G = 1$.

From the form of the metric, i.e. stationary and axis-symmetric, we can identify two Killing fields, namely ∂_t and ∂_ϕ [2]. The field ∂_t is time-like only on the exterior of the region characterised by the radius $2r_E(\theta) = r_s + \sqrt{r_s^2 - 4a^2cos(\theta)^2}$. This region is commonly referred to as the ergosphere. In addition to the ergosphere we find two singular surfaces at $\Delta(r) = 0$. We will restrict the study of geodesics to the exterior of the surface at the radius $2r_+ = r_s + \sqrt{r_s^2 - 4a^2}$, the inner surface being completely inaccessible.

A quick warning is always due when dealing with the Kerr metric: the spin parameter a of a Kerr black hole is connected to angular momentum. However, no solution of the Einstein field equations for a rotating, oblate mass density that matches the Kerr metric has been found yet [4]. Moreover, if we wish to avoid the possibility of naked singularities, the spin of a Kerr black hole must always be smaller than a half of the Schwarzschild radius.

After noting these points, we can proceed with the study of geodesic motion.

1.2 Conserved Quantities and Equations of Motion

To simplify the equations, it is useful to identify the constants of motion of the Kerr metric. By using the Killing fields and the conservation of the space-time interval we obtain three constants:

$$k \equiv \frac{1}{2}\mathcal{L}(\dot{x}, \dot{x}) \tag{2}$$
$$\epsilon \equiv (\partial_t, \dot{x}) \tag{3}$$
$$l \equiv (\partial_\phi, \dot{x}) \tag{4}$$

The physical interpretation of these constants will become more apparent in the study of equatorial geodesics. The constant k can be normalised to either 1 for massive particles or 0 for light rays.

There also exists a fourth conserved quantity, the Carter constant [5], which historically has proven more difficult to identify and interpret. The existence of four constants of motion for four variables make the problem of geodetic motion in a Kerr space-time fully integrable and thus easily solvable with numerical methods.

The analytical treatment of geodetic motion in Kerr space-time is very complex and generally not possible. We will make our life easier by starting with geodesics in the equatorial plane.

2 Equatorial Plane

From the special symmetry of the metric, we deduce that there exists a class of geodesics that are bound to the equatorial plane [3]. For such geodesics we set the angle $\theta = \pi/2$ and the angular velocity $\dot{\theta} = 0$. Restricting ourselves to the equator will allow us to reduce the problem to a single equation of motion.

First, we calculate the line element for the metric in the equatorial plane:

$$ds^2 = (1 - \frac{r_s}{r})dt^2 + 2a\frac{r_s}{r}dtd\phi - (r^2 + \frac{a^2(r+r_s)}{r})d\phi^2 - \frac{r^2}{a^2 + r^2 - rr_s}dr^2 \tag{5}$$

2.1 Radial Equation of Motion

We can obtain a first order differential equation for the radius r by eliminating the variables $\dot{\phi} = \dot{\phi}(r, \epsilon, l)$ and $\dot{t} = \dot{t}(r, \epsilon, l)$ from equation (2). Luckily enough we have found the constants of motion ϵ and l that let us do just that from equations (3) and (4):

$$\dot{\phi} = \frac{a\epsilon r_s - l(r - r_s)}{ra^2 + r^2(r - r_s)} \tag{6}$$

$$\dot{t} = \frac{\epsilon r^3 + alr_s + a^2\epsilon(r + r_s)}{ra^2 + r^2(r - r_s)} \tag{7}$$

$$\implies k = \frac{r^3(\epsilon^2 - \dot{r}^2) + 2a\epsilon lr_s - l^2(r - r_s) + a^2\epsilon^2(r + r_s)}{2ra^2 + 2r^2(r - r_s)} \tag{8}$$

We would like to arrange equation (8) in the form of a relativistic energy conservation equation in a potential: $\frac{1}{2}\dot{r}^2 = E - V_{eff}(r)$, where we define a total energy E and an effective radial potential $V_{eff}(r)$.

With some computation, the radial equation of motion becomes:

$$\frac{1}{2}\dot{r}^2 = \epsilon^2 - k + \frac{kr_s}{r} + \frac{a^2(\epsilon^2 - k) - l^2}{r^2} + \frac{a^2\epsilon^2 r_s + 2a\epsilon lr_s + l^2 r_s}{r^3} \tag{9}$$

From which we recognise the total energy E and the effective potential V:

$$E_k \equiv \epsilon^2 - k \tag{10}$$

$$V_{eff}(r) \equiv -k\frac{r_s}{r} + \frac{l^2}{r^2} - r_s\frac{l^2}{r^3} - a^2\frac{\epsilon^2 - k}{r^2} - a\frac{2\epsilon lr_s}{r^3} - a^2\frac{\epsilon^2 a^2 r_s}{r^3} \tag{11}$$

We can immediately distinguish Schwarzschild and Kerr terms in the effective potential (11) by taking the limit $a \to 0$. From this limiting case we also recover the interpretation of the constant l as the conserved angular momentum of the geodesic. We can see a typical plot of the effective potential in Figure (1).

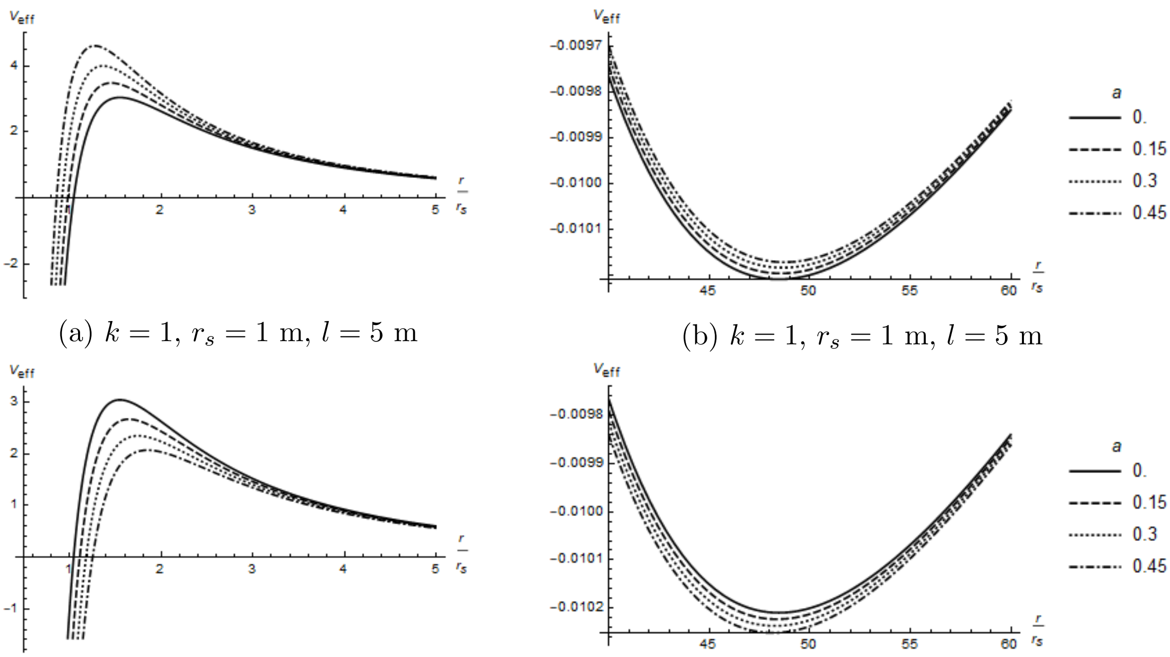

(a) $k = 1$, $r_s = 1$ m, $l = 5$ m

(b) $k = 1$, $r_s = 1$ m, $l = 5$ m

(c) $k = 1$, $r_s = 1$ m, $l = -5$ m

(d) $k = 1$, $r_s = 1$ m, $l = -5$ m

Figure 1: *Behaviour of the effective potential near to the extremal points for different choices of parameters. The solid black lines are identical in both plots.*

Notice how the behaviour is dependant on the relative direction of the orbital angular momentum and the black hole spin. This will also have an effect on the radius of the circular orbits, which are the topic of the next section.

2.2 Circular Equatorial Orbits

The simplest results that we can derive from the effective potential are the radii of the possible circular orbits around a Kerr black hole. We will denote them with r_0 for null and $r_\pm$ for time-like geodesics.

To obtain the radii, we have to set the derivative of the effective potential to zero:

$$\partial_r V(r) = 0 \text{ ; for } k = 0, 1$$

Which will give us an equation for the radius r. From this point on, we will separate the null and the time-like cases for the sake of clarity.

After some computation we obtain the results:

$$r_0 = \frac{3}{2} r_s \frac{l + a\epsilon}{l - a\epsilon} \tag{12}$$

$$r_\pm = \frac{l^2 - a^2 E}{r_s} \pm \sqrt{-3(a\sqrt{E+1} + l)^2 + \frac{(l^2 - a^2 E)^2}{r_s^2}} \tag{13}$$

Which we can compare to the well known Schwarzschild solutions by linearising in the spin parameter a:

$$r_0 \approx \frac{3}{2} r_s + 3\epsilon r_s \times \frac{a}{l} + \mathcal{O}[(\frac{a}{l})^2]$$

$$r_\pm \approx \frac{l^2}{r_s}(1 \pm \sqrt{1 - 3\frac{r_s^2}{l^2}}) \mp \frac{3\sqrt{E+1} r_s}{\sqrt{l^2 - 3r_s^2}} \times \frac{a}{l} + \mathcal{O}[(\frac{a}{l})^2]$$

We can recognise the Schwarzschild circular orbit in the zero order terms in the expansion and observe the behaviour of the full solution in Figure (2):

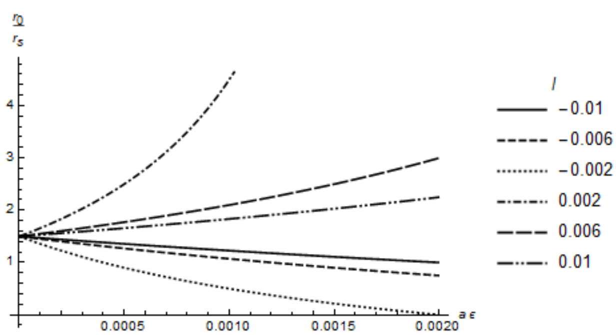

(a)

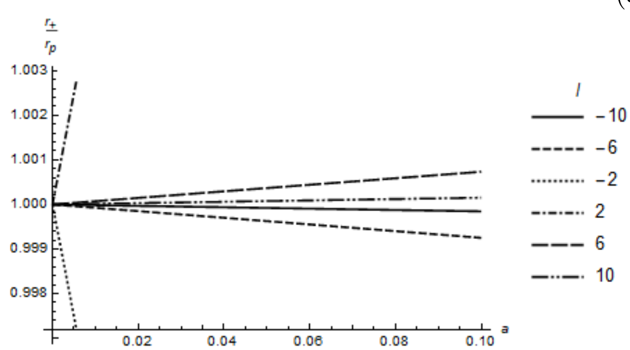

(b)

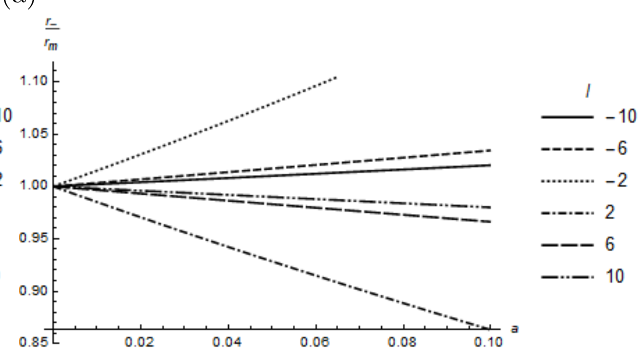

(c)

Figure 2: *Behaviours of the different solutions for the circular orbits. Plot 2.a is normalised with the schwarzschild radius whereas plots 2.b and 2.c are normalised with the respective schwarzschild outer and inner circular orbits.*

We observe that the larger the orbital angular momentum, the less relevant the Kerr correction becomes. This makes sense, as a larger angular momentum corresponds to a larger radius, which is less influenced by non Newtonian terms in the effective potential.

For a light ray orbiting the black hole in opposite direction to the spin, some peculiar circular orbits exist inside the ergo-sphere. We will however not analyse these any further and instead take the next step to finding a more general solution to the radial equation of motion.

2.3 Harmonic Approximation

Equation (9) is too complicated to solve analytically. A possible way to tackle the problem is to linearise the metric and then proceed to perturb around a Newtonian ellipse, just as one would do for the Schwarzschild case. An other possibility is to take the effective potential and expand it around a minimum to obtain a harmonic approximation. We have chosen the latter approach.

To find the minima in the effective potential, we have to assure that the second derivative of the effective potential be positive. From this condition, we expect to find some relations between the different parameters of the geodesic and of the black hole. We can reduce the condition of a minimum in the potential to the following statements:

$$\partial_r^2 V(r)|_{r=r_0} > 0 \implies |l| < a|\epsilon| \qquad \text{for } k=0 \tag{14}$$

$$\partial_r^2 V(r)|_{r=r_+} > 0 \implies \epsilon < 0;\ [l = -\frac{a}{\epsilon}] \vee [r_s < \frac{1}{\sqrt{3}}\frac{l^2 - a^2 E}{l + a\epsilon}] \qquad \text{for } k=1 \tag{15}$$

$$\partial_r^2 V(r)|_{r=r_-} > 0 \implies \epsilon < -1;\ [|l| < a\sqrt{E}] \wedge [r_s < \frac{1}{\sqrt{3}}\frac{l^2 - a^2 E}{l + a\epsilon}] \qquad \text{for } k=1 \tag{16}$$

It turns out, that condition(16) is never satisfied for non over-extremal black hole with $a < 0.5 r_s$. Condition (14) in turn leads to a negative value for the supposed stable radius. this leaves us only with one case which may be satisfied with the correct choice of parameters.

We thus have found that there exists only one stable circular orbit around a non over-extremal black hole at the radius r_+. It corresponds to the stable orbit in the Schwarzschild limit $a \to 0$.

Now, let's proceed with the approximation of the equation of motion (9) by replacing the radius with a circular orbit r_C plus a small perturbation δr:

$$\frac{1}{2}\dot{\delta r}^2 = E - V(r_C + \delta r) \approx E - V(r_C) - \frac{\delta r^2}{2}\partial_r^2 V(r)|_{r=r_C} + \mathcal{O}[\delta r^3]$$

By defining the energy of the harmonic oscillation $E_H \equiv 2E_k - 2V(r_C)$ and separating the variables, we obtain:

$$\frac{d\delta r}{d\lambda} = \sqrt{E_H - \partial_r^2 V(r)|_{r=r_C}\delta r^2}$$

Which has the solution:

$$r(\lambda) = r_C + A\sin(\omega\lambda - \psi_0) \tag{17}$$

$$A = \sqrt{\frac{E_H}{\partial_r^2 V(r)|_{r=r_C}}} \tag{18}$$

$$\omega = \sqrt{\partial_r^2 V(r)|_{r=r_C}} \tag{19}$$

For such a harmonic motion to be allowed, the energy of the oscillator must be positive. We therefore gain another condition that goes together with condition (15):

$$E_H|_{r=r_+} > 0 \implies E + \frac{r_s^2}{4l^2} + \mathcal{O}[(\frac{r_s}{l})^4] > 0 \tag{20}$$

At this point, we have to introduce the main approximations that will be often used in the rest of this work: the Semi-Newtonian limit $l \gg r_s$. It corresponds to an orbit that is only slightly affected by the effects that would occur near to the black hole. In this limit we expect the solutions for the geodesic to closely resemble ellipses.

2.3.1 Massive Particle, Semi-Newtonian Limit, Outer Solution

By combining (13) and (19) and taking the limit for large l, we obtain the final condition for a stable harmonically oscillating orbit:

$$-\frac{r_s^2}{4l^2} < E < 0 \wedge a < \frac{|l|}{\sqrt{E+1}} \tag{21}$$

These conditions are always met if the total energy of the orbit is negative and very small and if the black hole is not over-extremal. To simplify further calculations it will be useful to define a new parameter $0 > e > 1$ that describes the energy through the following equation.

$$E = -e^2 \frac{r_s^2}{4l^2} \tag{22}$$

In this limit and using these conditions, we can analyse the amplitude of the oscillation with respect to the circular orbit and the frequency of the oscillation with respect to the circular orbital frequency:

$$\frac{A}{r_+} \approx e + \mathcal{O}[e^2 \frac{r_s}{l}] \tag{23}$$

$$\frac{\omega}{\dot{\phi}|_{r=r_+}} \approx 1 - \frac{3r_s^2}{4l^2} - a\frac{r_s^2}{l^3} - \frac{4a^2(4-e^2)r_s^2 + 27r_s^4}{32l^4} + \mathcal{O}[(\frac{r_s}{l})^5] \tag{24}$$

From equation (23) we see that we can make the amplitude of oscillation as small as we want by choosing an orbit with a small energy parameter e. In fact, for a very small parameter e we can approximate a precessing ellipse with low eccentricity! If the angular velocity is approximately constant and the affine parameter is proportional to the proper time, or $\phi(t) \approx \omega t \propto \omega\lambda$, we obtain :

$$\frac{r(\lambda)}{r_+} = 1 - e\cos(\omega\lambda) \approx \frac{1}{1 + e\cos(\omega\lambda)} \approx \frac{1}{1 + e\cos(\phi)}$$

which has the form of an ellipse with orbital frequency ω and ellipticity e.

We observe the perihelion precession by looking at the extra terms in equation (24).The the most relevant term of the precession is a Schwarzschild effect of second order whereas the Kerr metric contributes with a term in third order. Higher order corrections are present both in a pure Schwarzschild black hole as well as due to the spin.

Collecting all of these results we see that semi-Newtonian equatorial orbits are in fact precessing ellipses, with a modified precession term.

3 Azimuthal Perturbations

After having dealt with the equatorial plane, we want to further our analysis to the azimuthal angle. If we take a closer look at the metric (1), we can notice that it depends on the angle θ only in quadratic order around the equatorial plane $\theta = \pi/2$. This means that we can analyse the equations of motion in first order without recurring to the Carter constant, as the θ dependence of the constants of motion (3) and (4) defined previously on vanishes.

3.1 Equation of Motion

We would like to obtain an equation of motion for the angle θ that only has linear terms. If we try to use the Lagrangian approach as we did for the radial equation (9) we will end up with an equation of motion that is quadratic in $\dot{\theta}$. This defeats the proposition of linearising the metric to avoid the Carter constant.

We therefore use the geodesic equation $\ddot{\theta} = \Gamma^{\theta}_{\mu\nu}\dot{x}^{\mu}\dot{x}^{\nu}$ and trade a quadratic first order differential equation for a linear second order differential equation.

To use the geodesic equation we have to calculate the relevant linearised Christoffel symbols. We set the angle $\theta = \pi/2 + \eta\delta\theta$ with a small parameter η. Moreover, we linearise the radius around a stable orbit $r_c + \eta\delta r$. We eliminate the cross terms $\delta\theta \times \delta r$ which are considered to be of quadratic order in η. This leads us to the following equation of motion:

$$\ddot{\delta\theta} = C_r\dot{\delta r} + C_\theta\delta\theta \tag{25}$$

Here we have defined the constant coefficients $C_r = C_r(r_s, a, l, \epsilon; r_c)$ and $C_\theta = C_\theta(r_s, a, l, \epsilon; r_c)$ according to the results of the linearisation. These coefficients are very complicated and are better studied within certain limits corresponding to previous results.

If we look at the form of equation (25), we recognise a harmonic oscillator in θ with a natural frequency ($\sqrt{|C_\theta|}$ and a drive term proportional to the radial velocity.

Before tackling the full problem, let's solve the case for $\dot{\delta r} = 0$, which corresponds to a circular orbit.

3.1.1 Inclined Spherical Orbit:

Lets fix the radius to be the only stable orbit r_+ we have found in the previous parts. The equation of motion (24) reduces to a simple harmonic oscillator, which we can solve by setting the initial conditions for the amplitude A_θ and the phase $\theta(0) = A_\theta$. We obtain:

$$\theta(\lambda) = A_\theta \cos(\sqrt{|C_\theta|}\lambda) \tag{26}$$

If we compare the orbital frequency and the frequency of the azimuthal perturbation we find:

$$\frac{\sqrt{|C_\theta|}}{\dot{\phi}|_{r=r_+}} = 1 + \frac{a^2(2E+3)r_s^2}{8l^4} + \mathcal{O}[(\frac{r_s}{l})^5] \tag{27}$$

As in the case for the radial oscillation, we find a precession term in the expansion. This is however a purely Kerr effect of fourth order known as the Lense-Thirring precession [6]. Due to the spin of the black hole, the orbital plane will slowly precess around the symmetry axis, which results in the precession term we see in equation (27)

3.2 Full Linearised Solution

Having characterised the azimuthal oscillation we go back and take a closer look at the driving term in equation (25), which is proportional to the radial velocity.

We have seen that the metric depends on the angle θ only quadratically. Therefore we expect the radial equation of motion to be unchanged in linear order. This means that we can use the harmonic solution of the radial equation of motion (15) and plug it in equation (25) to obtain:

$$\ddot{\delta\theta} = C_r A_r \omega_r \cos(\omega_r \lambda - \psi_0) + C_\theta \delta\theta \tag{28}$$

$$\implies \delta\theta(\lambda) = C_1 \cos(\omega_\theta \lambda) + C_2 \sin(\omega_\theta \lambda) + A_r C_r \omega_r \frac{\cos(\omega_r \lambda - \psi_0)}{\omega_\theta^2 - \omega_r^2} \tag{29}$$

This is an equation describing a resonating harmonic oscillator. As we guessed before, we can identify the natural frequency ω_θ and the driving frequency ω_r. The parameters C_1 and C_2 are constants of integration that will be eliminated by choosing initial conditions. The parameter ψ_0 describes the phase difference between the radial and the azimuthal oscillation.

Lets choose the initial conditions, so that the perturbation is extremal at $\lambda = 0$:

$$\delta\theta(0) = A_\theta \implies C_1 = A_\theta - A_r C_r \omega_r \frac{\cos(\psi_0)}{\omega_\theta^2 - \omega_r^2}$$

$$\dot{\delta\theta}(0) = 0 \implies C_2 = -A_r C_r \omega_r^2 \frac{\sin(\psi_0)}{\omega_\theta(\omega_\theta^2 - \omega_r^2)}$$

If we plug the coefficients back in the equation, we indeed observe that the amplitude of the harmonic components depend on the phase parameter ψ_0. Moreover, the drive term is controlled by the amplitude A_3, which we expect to vanish for a non rotating black hole.

$$\delta r(\lambda) = A_r \sin(\omega_r \lambda - \psi_0) \tag{30}$$

$$\delta\theta(\lambda) = A_1(\psi_0)\sin(\omega_\theta \lambda) + A_2(\psi_0)\cos(\omega_\theta \lambda) + A_3 \cos(\omega_r \lambda - \psi_0) \tag{31}$$

With the coefficients:

$$A_1 = -\frac{A_r C_r \omega_r^2 \sin(\psi_0)}{\omega_\theta(\omega_\theta^2 - \omega_r^2)} \tag{32}$$

$$A_2 = A_\theta - \frac{A_r C_r \omega_r \cos(\psi_0)}{\omega_\theta^2 - \omega_r^2} \tag{33}$$

$$A_3 = \frac{A_r C_r \omega_r}{\omega_\theta^2 - \omega_r^2} \tag{34}$$

The value of ψ_0 may be chosen freely. It describes all the possible orientations of an orbit. Two natural choices would be $\psi_0 = 0$ and $\psi_0 = \pi/2$, which correspond to an out of phase and an in phase oscillation respectively. An out of phase orbit has both aphelion and perihelion crossing the equatorial plane, whereas if $\psi_0 = \pi/2$, aphelion and perihelion will be the points furthest from the equatorial plane. We will analyse both cases separately, but before, let us compute the magnitudes of the relevant coefficients for a semi-Newtonian orbit by reintroducing the square eccentricity p:

$$A_3 = \frac{ar_s\sqrt{|p|}}{3l} + \mathcal{O}[(\frac{r_s}{l})^2] \tag{35}$$

$$\frac{\omega_\theta}{\dot{\phi}|_{r=r_+}} = 1 + 3\frac{a^2r_s^2}{8l^4} + \mathcal{O}[(\frac{r_s}{l})^5] \tag{36}$$

$$\frac{\omega_r}{\dot{\phi}|_{r=r_+}} = 1 - \frac{3r_s^2}{4l^2} - a\frac{r_s^2}{l^3} - \frac{4a^2(4+p)r_s^2 + 27r_s^4}{32l^4} + \mathcal{O}[(\frac{r_s}{l})^5] \tag{37}$$

$$\frac{\omega_\theta - \omega_r}{\dot{\phi}|_{r=r_+}} = \frac{3r_s^2}{4l^2} + a\frac{r_s^2}{l^3} + 3\frac{a^2r_s^2}{8l^4} + \frac{4a^2(4+p)r_s^2 + 27r_s^4}{32l^4} + \mathcal{O}[(\frac{r_s}{l})^5] \tag{38}$$

$$\frac{\omega_\theta + \omega_r}{\dot{\phi}|_{r=r_+}} = 2 - \frac{3r_s^2}{4l^2} - a\frac{r_s^2}{l^3} + 3\frac{a^2r_s^2}{8l^4} - \frac{4a^2(4+p)r_s^2 + 27r_s^4}{32l^4} + \mathcal{O}[(\frac{r_s}{l})^5] \tag{39}$$

We immediately see that the amplitude of the driving term vanishes if we set $a = 0$. Moreover, just like the radial oscillation, the magnitude of A_3 is controlled by the eccentricity of the geodesic. Looking at the other terms, we recognise the ellipse precession term coming from the Schwarzschild metric, the ellipse precession term coming from the Kerr metric and the orbital plane precession term, also coming from the Kerr metric:

$$\Delta\phi_S \equiv \frac{3r_s^2}{4l^2} \tag{40}$$

$$\Delta\phi_K \equiv a\frac{r_s^2}{l^3} \tag{41}$$

$$\Delta\theta \equiv 3\frac{a^2r_s^2}{8l^4} \tag{42}$$

Now lets take a closer look at the two special cases.

3.2.1 In and Out of Phase Oscillations

If we set set ψ_0 to 0. Equation (30) and (31) simplify to:

$$\delta r(\lambda)|_{\psi_0=0} = A_r \sin(\omega_r\lambda) \tag{43}$$

$$\delta\theta(\lambda)|_{\psi_0=0} = A_\theta \cos(\omega_\theta\lambda) + 2A_3 \sin(\frac{\omega_\theta - \omega_r}{2}\lambda)\sin(\frac{\omega_\theta + \omega_r}{2}\lambda) \tag{44}$$

If we instead set ψ_0 to $\pi/2$. Equation (30) and (31) simplify to:

$$\delta r(\lambda)|_{\psi_0=\pi/2} = A_r \cos(\omega_r\lambda) \tag{45}$$

$$\delta\theta(\lambda)|_{\psi_0=\pi/2} \approx A_\theta \cos(\omega_\theta\lambda) + 2A_3 \sin(\frac{\omega_\theta - \omega_r}{2}\lambda)\cos(\frac{\omega_\theta + \omega_r}{2}\lambda) \tag{46}$$

For equation (46) we have used the fact that the ratio of radial and azimuthal perturbation is 1 up to quadratic order in the usual expansion. We can plot a typical solution to visualise the in and out of phase cases in Figure (3), where we have collected the terms arising from the Kerr metric the modulation contribution $M(\lambda)$:

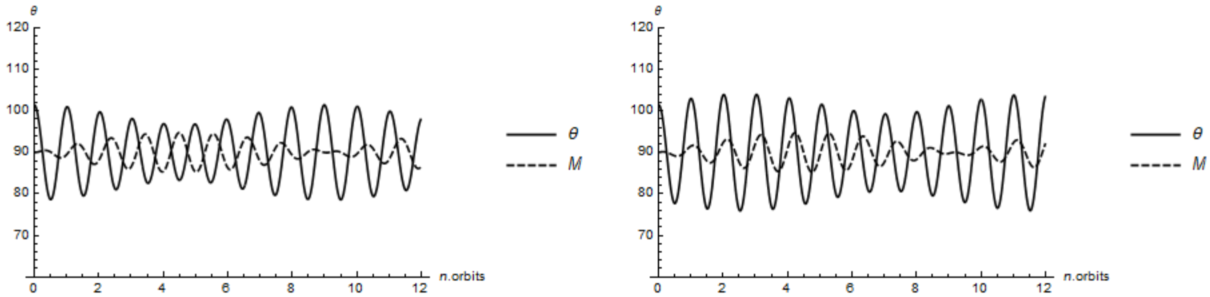

(a) $\psi = 0$ (b) $\psi = \pi/2$

Figure 3: *Solution of the azimuthal angle for in and out of phase special cases plotted as a function of the number of completed revolutions around the black hole. The parameters of the plot have been chosen to maximise the visibility of the effects, without changing the qualitative behaviour of the system. In this case $r_s = 1$ m, $a = 0.5$ m and $l = 4$ m. The energy parameter e has been chosen to be 1. Also plotted is the contribution of the modulation M to the angle.*

From the equations and the plots, we see that the Kerr metric couples the azimuthal and the radial oscillation through the parameter a contained in the amplitude A_3. The effect results in a modulated oscillation of the angle θ over the course of many orbits.

By noting that all relevant frequencies are described in terms of the various precession terms, we deduce that the physical reason for this modulation is the interplay between the ellipse precession and the orbital plane precession. Such an interplay is only possible in the Kerr metric, as there is no precession of the orbital plane in the Schwarzschild case.

By comparing the out of phase solution in Figure (3.a) and the in phase solution in Figure (3.b) we see how the modulation is effectively changing the maximal amplitude of the natural harmonic oscillation over the course of many orbits. We will analyse this effect in the next subsection.

3.2.2 The Effective Amplitude

Following the consideration in section 3.2.1, we rewrite the solution for θ as a harmonic oscillation with λ dependant amplitude:

$$\delta\theta(\lambda) \approx A_{\text{eff}}(\lambda)\cos(\omega_\theta \lambda) \tag{47}$$

This term fully describes the variation of the solution from a harmonic oscillation with a natural frequency ω_θ. By using a few trigonometric identities and following the usual procedures to create an envelope of a signal, equation (44) can be transformed into an expression for the effective amplitude. It turns out that this transformation only works nicely for the out of phase orbit and we will concentrate on that one only:

$$A_{\text{eff}} = A_\theta + A_3\left(\frac{\cos(\omega_r\lambda)}{\cos(\omega_\theta\lambda)} - 1\right) \approx A_\theta - A_3\sin^2((\omega_\theta - \omega_r)\lambda) \qquad \text{for } \psi_0 = 0 \tag{48}$$

A plot of the envelope can be seen in Figure (4):

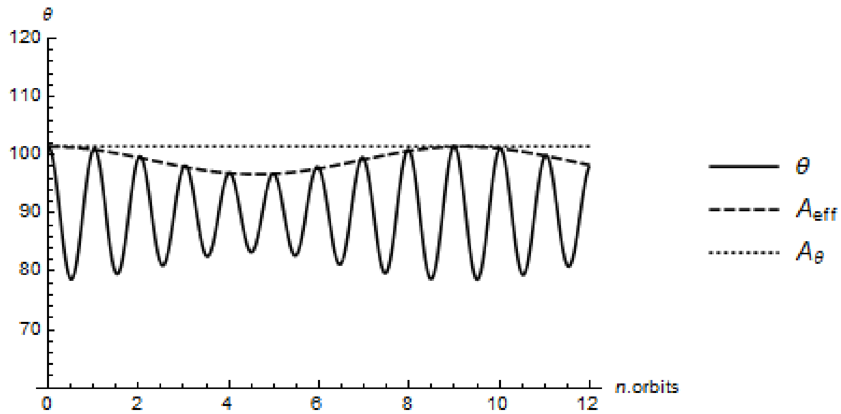

Figure 4: *Plot showing how a squared sinus effective amplitude envelopes the oscillation in the out of phase case. In this plot $r_s = 1$ m, $a = 0.5$ m and $l = 4$ m. The energy parameter e has been chosen to be 1 to maximise the effect of the modulation.*

With this description, it becomes apparent (at least in the $\psi_0 = 0$ case) what the physical effect of the modulation is: it introduces a rocking motion around the equatorial plane with a frequency of $\omega_\theta - \omega_r \propto \Delta\phi_S + \Delta\phi_K$. So as the ellipse itself and the orbital plane precess, the orbital plane also oscillates in its angle respective to the equatorial plane at the same rate at which the precession of the ellipse occurs. We can elegantly describe this effect as a complex precession of the angular momentum vector, as we will see in section 4.3.

4 The Perturbed Outer Time-like Geodesic

4.1 Linearisation of the Polar angle and of the Time Coordinate

We now have found an analytic, perturbed solution around the outer stable circular orbit of a Kerr black hole for the radial and the azimuthal coordinate. To complete the geodetic solution we have to solve the equations for ϕ and t also. We use equations (3) and (4) to find expressions for $\dot{\phi}$ and $\dot{t}$ which we can linearise in the radial perturbation and in the azimuthal perturbation, just as we did until now. Moreover, we take the usual limit of semi-Newtonian. The equations simplify in a way that is not too surprising:

$$\dot{\phi} \approx (1 - \frac{r_s}{l^2}\delta r) \times \dot{\phi}|_{r=r_+} \approx \text{ const. } \equiv \omega_o \tag{49}$$

$$\dot{t} \approx (1 - \frac{r_s^3}{4l^4}\delta r) \times \dot{t}|_{r=r_+} \approx \text{ const.} \tag{50}$$

We can see, that the corrections of the rates of change of the two other coordinates are of higher order in our semi-Newtonian limit. We can safely set them to a constant value, namely the value they would have if the orbit were circular.

4.2 The Solution

After all these considerations we are finally ready to present a solution to the geodesic equations in Kerr space-time, valid close to the stable equatorial circular orbit, computed in a semi-Newtonian limit:

$$t(\lambda) = \dot{t}|_{r=r_+}\lambda + t_0 \tag{51}$$
$$r(\lambda) = r_+ + A_r \sin(\omega_r\lambda - \psi_0) \tag{52}$$
$$\phi(\lambda) = \omega_o\lambda + \phi_0 \tag{53}$$
$$\theta(\lambda) = \frac{\pi}{2} + A_1(\psi_0)\sin(\omega_\theta\lambda) + A_2(\psi_0)\cos(\omega_\theta\lambda) + A_3\cos(\omega_r\lambda - \psi_0) \tag{54}$$

Where r_+ denotes the analytical stable circular orbit on the equatorial plane, ω_o the orbital frequency at that radius and $t(\lambda) = \dot{t}|_{r=r_+}$ the rate of change of time at that radius. The coefficients A_r and $A_{1,2,3}$ are dependent on the parameters of the black hole and of the orbit. The trivial free parameters of this solution are the initial time t_0 and the initial angle ϕ_0. The only important free parameter is the phase ψ_0, which governs the interactions between the radial and the azimuthal oscillations.

4.3 The Precession of the Angular Momentum Vector

In the previous sections, we have seen how the driving term in equation (25) affects the behaviour of the angle θ: the orbital plane oscillates in its angle with respect to the equatorial plane. To quantify and interpret this effect it is very useful to take a look at the angular momentum vector of the orbit.

$$\vec{L} = \vec{r} \times \vec{v} \tag{55}$$

We can construct the position and the velocity vectors from our general solutions (51-54). Then obtain $\vec{L}$ by calculating the cross product. However we have to be careful: When talking about the angular momentum we have to remember that it is a conserved quantity only in the case of exact Newtonian mechanics. Moreover, our solution is only an approximation of an ellipse. This means that we expect the magnitude of the angular momentum defined in (55) to vary slightly as the particle travels through its orbit. This does not however broadly affect the precession of the angular momentum, as it occurs over many orbits.

We want to describe the orientation of the orbital plane. Therefore we are allowed to normalise the position and the velocity vectors. We replace $\vec{r} \to \vec{n}_r$ and $\vec{v} \to \vec{n}_v$ in equation (55) and normalise the angular momentum.

If we project the angular momentum unit vector back to the XY plane we should get an idea of the precession.

We can see the effects of the modulation very clearly in Figure (5): It introduces an additional nutation effect to the precession of the orbital plane. The nutation occurs essentially at the rate of the ellipse precession (see Section 3.2.1 and 3.2.2). We can now also understand what the effect of varying the phase ψ_0 is: namely it turns the graph of the precessing angular momentum vector anticlockwise as it increases from 0 to 2π (not shown in figure 5). Notice the fuzziness of the graphs: the very small scale features represent the small variations in the angular momentum magnitude occurring periodically every orbit.

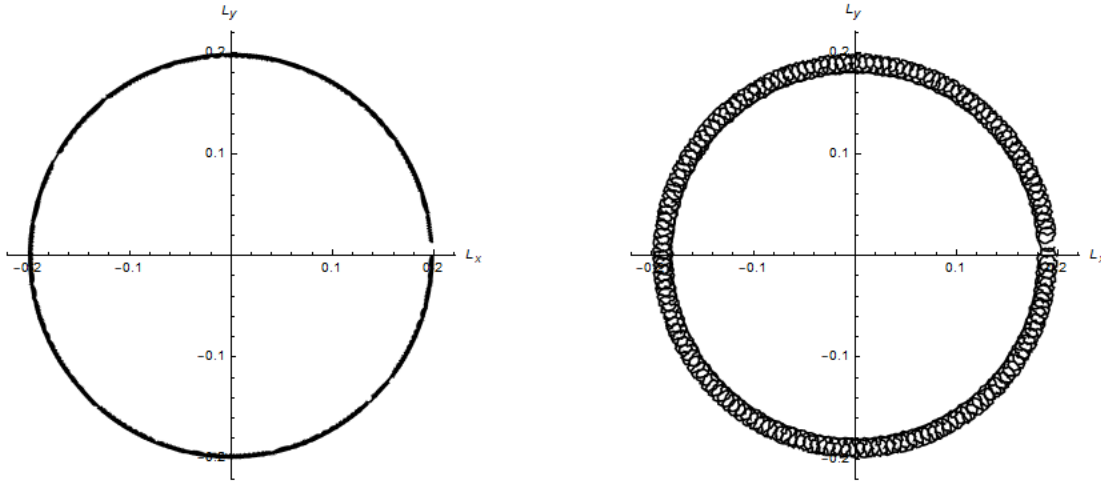

(a) *Circular* $p = 0$; $\psi = 0, \pi/2$ (b) *Elliptical* $p = 0.05$; $\psi = 0$

Figure 5: *Precession of the angular momentum vector projected on the plane. The parameters are chosen to make the effects visible but are in line with all approximations. In this plot* $r_s = 1$ *m,* $a = 0.5$ *m,* $l = 4$ *m,* $A_\theta \approx 11^o$*. The 'precession dance' takes over 2700 orbits to complete with these parameters.*

From these considerations we can compute an interesting number: the number small of twirls N_t during a full 2π precession of the angular momentum vector. This will simply be the ratio of the ellipse precession rate and the plane precession rate.

$$N_t \equiv \frac{\omega_r - 1}{\omega_\theta - 1} \approx 2\frac{l^2}{a} + \frac{8l}{3a} + \frac{4}{3} - \frac{e^2}{3} + \frac{9r_s^2}{4a^2} \tag{56}$$

For the parameters in Figure (5.b) we obtain about 160 twirls.

5 Conclusion

5.1 Brief Summary of Results

A few points can broadly sum up what we have found to be the behaviour of a semi-Newtonian, quasi-circular and quasi-equatorial stable geodesic with angular momentum l and eccentricity e around a Kerr black hole with Schwarzschild radius r_s and spin a.

- The orbit will precess in the plane with a modified precession term $\Delta\phi = \frac{3r_s^2}{4l^2} + a\frac{r_s^2}{l^3}$.
- The orbital plane will undergo a Lense-Thirring precession around the black hole spin axis with a precession term of $\Delta\theta = 3\frac{a^2 r_s^2}{8l^4}$
- The orbital plane will slightly oscillate on its intersection with the equatorial plane. This is equivalent to adding a nutation effect to the precession of the angular momentum unit vector. The amplitude of the nutation in the angle θ is $\frac{ar_s e}{3l}$ and the frequency is approximately equal the precession term of the ellipse $\Delta\phi = \frac{3r_s^2}{4l^2} + a\frac{r_s^2}{l^3}$.

5.2 Acknowledgements

Many thanks to Yannick Bötzel for giving me a good idea what to expect when dealing with orbits in space-time. A load of thanks to Stephen Wolfram for inventing Mathematica. Thanks to Seba just cause I told him I would thank him.

References

[1] R. Kerr,1963. Gravitational Field of a Spinning Mass as an Example of Algebraically Special Metrics,American Physical Society.

[2] G.Graf, 2017. General Relativity HS 2017 script, ETHZ.

[3] Pugliese et al. ,2011. Equatorial motion in Kerr spacetime, Universita' di Roma La Sapienza.

[4] G.Marsh. Rigid Rotation and the Kerr Metric, Argonne National Laboratory.

[5] B. Carter, 1968.Global Structure of the Kerr Family of Gravitational Fields, Phys. Rev. 174.

[6] C.Chakraborty, 2014. Strong gravity Lense-Thirring Precession in Kerr and Kerr-Taub-NUT spacetimes,Saha Institute of Nuclear Physics.